A re-analysis for the seasonal and longer-period cycles and the trends in middle atmosphere temperature from HALOE

Ellis E. Remsberg[1]

[1]Science Directorate, NASA Langley Research Ctr., Hampton

E. E. Remsberg, Science Directorate, Mail Stop 401B, NASA Langley Research Center, Hampton, VA 23681-2199. (e-mail: Ellis.E.Remsberg@nasa.gov)

Abstract.

Previously published analyses for the seasonal and longer-period cycles in middle atmosphere temperature versus pressure (or T(p)) from the Halogen Occultation Experiment (HALOE) are extended to just over 14 years and updated to properly account for the effects of autocorrelation in its time series of zonally-averaged data. The updated seasonal terms and annual averages are provided, and they can be used to generate temperature distributions that are representative of the period 1991-2005. QBO-like terms have also been resolved and are provided, and they exhibit good consistency across the range of latitudes and pressure-altitudes. Further, exploratory analyses of the residuals from each of the 221 time series have yielded significant 11-yr solar cycle (or SC-like) and linear trend terms at a number of latitudes and levels. The amplitudes of the SC-like terms for the upper mesosphere agree reasonably with calculations of the direct solar radiative effects for T(p). Those SC amplitudes increase by about a factor of 2 from the lower to the upper mesosphere and are also larger at the middle than at the low latitudes. The diagnosed cooling trends for the subtropical latitudes are in the range, -0.5 to -1.0 K/decade, which is in good agreement with the findings from models of the radiative effects on pressure surfaces due to known increases in atmospheric CO2. The diagnosed trends are somewhat larger than predicted with models for the upper mesosphere of the northern hemisphere middle latitudes.

1. Introduction

Time series of zonal-average temperature versus pressure or T(p) from the Halogen Occultation Experiment (HALOE) were analyzed for their seasonal and longer-period terms in the upper stratosphere and mesosphere, as reported in *Remsberg et al.* [2002a] and *Remsberg and Deaver* [2005]. HALOE made its last measurements on November 21, 2005, and its parent UARS spacecraft was de-activated in mid December 2005. The seasonal and interannual terms reported by *Remsberg et al*. [2002a] were based on 9.5 years of data; the results in the present paper are based on just over 14 years of data. The longer-period terms in *Remsberg and Deaver* [2005] were based on 12.5 years of data, and those analyses are now extended to 14 years, too. More importantly, it has been learned that the analyses in *Remsberg et al.* [2002a] and *Remsberg and Deaver* [2005] did not account properly for the effects of autoregression in those time series of zonal-average T(p). As a result, the amplitudes that they reported for the seasonal and longer-period terms were underestimated. They also had some difficulty with the fitting of an underlying trend term in the presence of a significant 11-yr solar cycle (SC) term. At times their fitted SC terms were not quite in-phase with the variations of the solar flux either.

The re-analyses herein account for the first order autoregression (AR1) term properly, leading to more accurate seasonal and longer-period terms. Terms are reported for ten-

degree wide latitude zones from 60S to 60N and for pressure levels from 3 hPa to 0.007 hPa. Terms were generated for some additional levels, too—1.5, 0.7, 0.15, 0.07, and 0.015 hPa. A total of 221 separate time series were analyzed, and the results were then checked for coherence with latitude and pressure altitude. The zonal mean and seasonal values can be used to generate a climatology of T(p) that is representative of the time span of October 1991 through November 2005. Section 2 reviews the updates that were applied to the original method of analysis. Section 3 contains a tabulation of the findings for the seasonal and then the longer-period and the linear trend terms. Phase anomalies from the earlier studies have been corrected now in most cases. The longer-period and trend terms from HALOE are also briefly compared with some other published results from datasets and from models. Section 4 is a summary of the findings herein from the time series of the HALOE T(p) data.

2. Time Series Re-analysis Approach

The procedure for assembling the time series of zonally-averaged sunrise (SR) and sunset (SS) points from the HALOE Version 19 (V19) Level 2 profiles is unchanged from that described in *Remsberg and Deaver* [2005] and references therein. For example, Figure 1 is an update of their original plot for 30N and 0.02 hPa (near 74 km). The SR (open) and SS (solid) points have been adjusted for the average diurnal variation at SR versus SS, as before. Multiple linear regression (MLR) techniques are used for fitting the significant polynomial and periodic terms to the time series data. The terms for Figure 1 include annual (AO), semiannual (SAO), and quasi-biennial oscillation (QBO of average period 852-dys) terms, an assumed 11-yr SC (or 4015-dy) term, and a linear trend term. As before, the periods and phases of the QBO and/or interannual (IA) terms are determined by a Fourier fit to the residuals after accounting for the seasonal terms. Only those terms that have been found to be highly significant are retained for the final MLR model of a given latitude and pressure level. For these reasons, separate analyses have been conducted for each level and latitude zone. The fit to the points for the combination of all the re-analyzed terms of Figure 1 is shown by the oscillating curve. The straight line fit is based on just the constant and linear trend terms.

Because the zonal mean data at time n have considerable memory of the atmospheric state from the previous point at n-1, the data time series have autoregressive

characteristics. The correct MLR result for that situation is obtained by a two-step process (see Appendix A of *Tiao et al.* [1990]). Initially, a model of the form,

$$T(n) = a + bX + e \sin(Z) + f \cos(Z) + \ldots + N(n), \qquad (1)$$

is used, where T(n) is the temperature at the n^{th} point in the time series. The model has a constant term 'a' and a linear term in $X = (t_n - t_1) / T$, where t_n is the time of the n^{th} observation point, t_1 is the first point in the time series, T is the total length of the time series, and b is the coefficient of the linear term. The model also has seasonal and longer-period terms that are represented by their Fourier components in Z, where $Z = 2\pi t_n / P$, and P is the period of a given cycle. Periodic terms that are considered are AO, SAO, QBO (and/or other interannual periods), and an 11-yr SC-like term. Only those terms with a significance of 85% or greater have been retained for the final models. Note that the seasonal terms almost always have a significance of greater than 99%. Finally, the term N(n) is the autoregressive (AR) noise residual that is given by

$$N(n) = \varphi N(n-1) + E(n), \qquad (2)$$

for a first order (AR1) process. The factor φ is the autocorrelation of the noise residual and E(n) is the white noise component. In practice, the estimates of φ are based on the residuals that are found from a fit of the dominant seasonal (AO and SAO) terms. Thus, the current MLR method consists of a fit for the seasonal terms of Eq. (1) and the generation of its model residuals N(n). A search is made for significant interannual terms

in N(n), and its autocorrelation coefficient φ is found. Then, a refitting is conducted for the complete set of transformed model terms of Eq. (3),

$$T(n) - \varphi\, T(n-1) = a\,[1-\varphi] + b\,[X(n) - \varphi\, X(n-1)] + \qquad (3)$$
$$e\,[\sin(Z(n)) - \varphi \sin(Z(n-1)] + f\,[\cos(Z(n)) - \varphi \cos(Z(n-1))] + \ldots + E(n).$$

Equation (3) has a more statistically valid, white noise residual E(n) and has the same coefficients as Eq. (1), except with different and now appropriate estimates of significance and uncertainty. It is noted that *Remsberg et al.* [2002a] (and *Remsberg and Deaver* [2005]) incorrectly fitted a slightly shifted (by one point) time series with itself, as indicated by the inclusion of a 'bT(n-1)' term in their Eq. (1). Their approach had the effect of reducing the variance of the model fit to the data and of reducing the coefficients of all the other terms for their MLR model fit. As a result, it was more difficult for them to resolve small amplitude terms and to find significant SC and linear trend terms. The present re-analysis employs the sequence of operations from Eq. (1) through Eq. (3) and yields more accurate results.

As an example, the re-analysis for 30N, 0.02 hPa is shown in Figure 1 and yields an autocorrelation coefficient φ of 0.34. The amplitude of the AO term is 6.9 K, which is larger than before by about 10%. There is also a significant QBO cycle of amplitude 0.8 K. The SC term has amplitude 2.1 K and its maxima occur in February of 1992 and 2003 or very near to those of the variations of the F10.7 cm solar flux. Note that this amplitude is analogous to a 'max minus min' variation of 4.2 K over the solar cycle. In addition,

there is a cooling trend term with a slope of -1.7 K/decade that is significant at the 99.8% level in the re-analysis. *Remsberg and Deaver* [2005] did not find a highly significant trend term for this level and latitude and their SC term had amplitude of only 1.7 K.

Table 1 and Figure 2 show the absolute values of the AR1 coefficient φ. Those values are generally small in the mesosphere, and, in fact, the signed values are occasionally negative in the subtropical upper mesosphere of the Southern Hemisphere and in the middle mesosphere at 10N. Small values for φ indicate very little memory for the time series points, even in a zonal mean sense. The smallest values occur in the middle mesosphere at subtropical latitudes, where the amplitudes of the seasonal cycles are also small compared with the effects of the tides and other wave activity for the measured temperatures. Values of φ are larger at the higher latitudes, where the amplitude of the annual cycle is increasing. Values of φ are also enhanced slightly in the middle mesosphere at the Equator, where the amplitude of the SAO term is large. It was expected that there would be larger values of φ in the stratosphere, and one can see that they increase from 1 to 3 hPa at most latitudes.

Prior to performing an MLR fit to the time series of the SS and SR data points, the means of the time series of just the SS points and then just the SR points were obtained, as in *Remsberg et al.* [2002a]. The two series of separate SS and SR points were adjusted by half the difference of those means. The purpose of this step was to make a first order adjustment for the effects of the tides in the retrieved HALOE T(p), prior to combining the SS and SR points into a single time series. That approach led to a better MLR fit (less

scatter) for the combined time series, which also had twice as many points as the two separate series. Table 2 contains the SS minus SR differences from those respective means, and they have a pattern with altitude at low latitudes that looks very similar to the predicted effects of the atmospheric diurnal tide. The largest differences occur in the Equatorial latitude zone and vary in sign (-8.3 K at 0.01 hPa and 7.0 K at 0.1 hPa) with about the expected vertical half-wavelength (16 km) of the diurnal tide. At 30 degrees latitude the apparent vertical wavelength has grown longer and its phase shifted, due presumably to the decline of the influence of the diurnal tide and to the added effects of the semi-diurnal tide [e.g., *Dudhia et al.,* 1993]. It should also be noted that the tropical SS/SR difference is small at 1.0 hPa, where a tidal maximum was expected. Just why the apparent effect of the diurnal tide is weak in the tropical upper stratosphere is unclear, although perhaps it is a result of obtaining annual average SS/SR differences and over the rather wide, 10-degree latitude zone.

A physically important characteristic of Table 2 is the large amount of symmetry in the mesosphere for the pattern and magnitude of the SS/SR differences between the two hemispheres, even at the latitude zones of 40 through 60 degrees where the effects of the 3-dy per year orbital precession and the changes for the seasonal sampling over the 14-yr period might be of some concern. Still, the differences at those higher latitudes zones are rather large (of order 5 K) near the stratopause and should be viewed with caution because of the subtle effects of that precession and of the marginal sampling rates for the large-amplitude, seasonal cycles from the SS and SR orbital segments. In fact, it could be argued that it is acceptable to perform a fit of the combined SS and SR series for those

higher latitudes without making a mean SS/SR adjustment. Instead, it was considered more important to be consistent in the data treatment across all latitudes and pressure-altitudes. As will be shown in the next section, the reanalysis results for the seasonal and longer-period terms from HALOE also exhibit good coherence across the range of latitudes and pressure-altitudes.

3. Results of the Re-analyses

a. Seasonal and Annual-Mean Terms

Table 3 and Figure 3 present the amplitudes of the annual cycles (AO) as a function of latitude and pressure-level. AO amplitudes are weak at the low latitudes and in the middle mesosphere at all latitudes. Much larger AO variations are found at the higher latitudes, especially near the stratopause and mesopause. As a result of properly accounting for the autoregressive effects in the zonal mean temperature data, it is noted that the AO amplitudes are larger than reported in *Remsberg et al.* [2002a] for those regions where the values of φ are relatively large. AO amplitudes are also similar for the same latitudes of each hemisphere, as expected. An exception occurs for the 30-40 degree latitude region, where the AO amplitudes in the upper mesosphere are larger in the NH than the SH. Conversely, the AO amplitudes of the SH are larger than in the NH for the lower mesosphere and upper stratosphere

Table 4 and Figure 4 contain the day or month of the year of the AO maximum, and there is excellent continuity in its timing across altitude and latitude. There is an out-of-phase relationship for the AO cycle at middle and high latitudes of the two hemispheres, indicating good seasonal symmetry for the AO. For example, at 1 hPa the AO maximum occurs on day 168 at 60N, while it is on day 344 at 60S, or 176 days (nearly 6 months) later. Even though the HALOE sampling occurs fairly infrequently at the higher latitudes, it appears to be adequate for resolving its large-amplitude AO cycles with good

accuracy. One can see the nearly 180-degree change in the AO phase that occurs in the middle mesosphere (between 0.10 and 0.15 hPa) for the higher latitudes. The AO phase is changing more gradually with altitude for the lower latitudes.

Table 5 and Figure 5 contain the average amplitude of the two SAO cycles. No attempt was made to distinguish between the first and second cycles, although it is likely that there are slight differences in their magnitudes and phases. There is more hemispheric similarity for the amplitudes for the SAO than for the AO. However, there is less certainty for the SAO than the AO amplitudes at 50 and 60 degrees of latitude because of the sparseness of the sampling from HALOE for at least one season. Table 6 contains the day of year for the temperature maximum in terms of its first SAO cycle, even though the SAO amplitudes and phases are obtained from the fit to both the first and second cycles of every year. As with the AO, there is good coherence for the timing of the SAO maximum with altitude and latitude.

The annual mean temperature distribution or constant term from the MLR analyses is given in Figure 6 and Table 7. This distribution together with the AO and SAO amplitude and phase information is all that one needs to assemble monthly or seasonal profiles of T(p) for scientific study. The annual mean and seasonal terms compare favorably with the values presented in *Barnett et al.* [1985], although the amplitude of their SAO term is significantly smaller in the mesosphere because of the much lower vertical resolution of their Pressure Modulated Radiometer (PMR) dataset. Because the QBO and SC-like terms have been obtained as part of the MLR fits for the seasonal

terms, one can be confident that the distributions of T(p) from Tables 3-7 are representative of the 1991-2005 period, at least within the known estimates of absolute error for the retrievals of the HALOE V19 temperature profiles [*Remsberg et al.,* 2002b]. There are several instances of likely bias in the HALOE temperatures of the upper mesosphere. The signal-to-noise (S/N) in its CO2 channel is becoming low at the level of 0.007 hPa, and there is a blending of its retrieved profile with that of the MSIS model. As a result, the temperature at that level is often a combination of the model and the measurement, based on a weighting for the two as determined by that S/N. It is also likely that the values at 60 degrees latitude for the levels of 0.007 and 0.01 hPa are affected by absorption from polar mesospheric cloud (PMC) particles during the summer months. This interference effect will lead to summer season and annual mean temperatures that are too warm by a few degrees [*McHugh et al.,* 2003]. The finite field-of-view (FOV) of the HALOE CO2 channel also tends to smooth the true amplitudes of the vertical structures in a temperature profile that have been induced by tides and/or by the breaking of gravity and planetary waves, particularly in the upper mesosphere [*LeBlanc and Hauchecorne*, 1997; *Remsberg et al.,* 2002b].

Figure 7 is the time series of T(p) and its MLR model fit for 60N and 0.007 hPa. The sampling is adequate for determining the AO, even at this high latitude. There are also significant SAO and SC-like terms of small amplitude at this level and latitude. The effects of the 3 day per year precession are clearly noticeable in the sequence of SR points to earlier times in the annual cycles from 1995 through 2001 during the revisits for the HALOE observations to this latitude. It is also noted that at this level there are effects

from the merging with the MSIS model during polar summer, when the S/N is low for the HALOE measurements of these coldest temperatures. It is also likely that some of the profiles include effects from PMCs, which would cause those minimum temperatures to be biased warm.

Table 8 gives the hemispheric differences (SH minus NH) for the annual mean temperatures. The subtropical upper mesosphere is slightly warmer in the SH than the NH. For the 40 through 60 degree latitude zones the SH annual means are warmer than in the NH in the upper mesosphere, which confirms the expected findings based on the model studies of *Siskind et al*. [2003]. At lower altitudes those HALOE differences are mostly negative. That finding is opposite to what Siskind et al. predicted, possibly because of the varying effects of the wave activity associated with the wintertime stratospheric warming events that they did not represent as well. Although the amplitude of the AO is larger in the upper mesosphere at 60 degrees latitude for the SH, the combination of the annual mean and the AO give summertime T(p) values that are colder in the NH. Such hemispheric differences imply that one ought to find more frequent occurrences of PMCs in the NH, as deduced from separate analyses of HALOE T(p) at high latitudes in *Hervig and Siskind* [2005].

b. Interannual Terms

The seasonal residuals were Fourier-analyzed for QBO and/or other interannual (IA) terms, rather than employing a proxy term based on the QBO wind oscillation of the tropical lower stratosphere. In a 14-yr dataset one can expect to find 6 to 7 complete

cycles. When any interannual terms were found to be highly significant, they were included in the MLR model. As an example, Figure 8 is the time series and model fit for 20S and 3 hPa. Its MLR model includes a significant linear trend term, a QBO-like term of period 853 days, and an IA term of period 640 days, as well as seasonal and SC terms. There does not appear to be much scatter for the points of the time series; the AR coefficient φ for the residuals of the seasonal model is 0.39. Because of the proper accounting for the AR effects in the present analysis, the amplitude of the QBO term is 0.6 K rather than the value of 0.3 K that was reported previously in *Remsberg et al*. [2002a]. The model also contains an accompanying, significant IA term of amplitude 0.4 K.

Table 9 shows the amplitudes of the dominant QBO or IA terms at each level and latitude, at least where those terms are significant. IA terms that have shorter periods (or in the range of 635 to 730 days) are denoted in Table 9 with an asterisk. Generally, the QBO and IA terms are of somewhat greater amplitude in the northern than the southern middle latitudes, and they are insignificant and absent throughout the mesosphere at most low latitudes. The predominant period in days for the QBO term varies slightly with latitude: 808 (60S), 839 (50S), 855 (40S), 854 (30S), 853 (20S), 835 (10S), 834 (Eq), 852 (30N), 853 (40N), 855 (50N), 855 (60N). But because the periods that are determined have an uncertainty of ±5 days, differences of that order are not considered significant. At 10N and 20N an IA term has amplitude that is larger than the QBO term, and the IA period is 639 days. Of equal importance are the phases for the QBO and IA terms, which are determined by the Fourier fit to the residuals. The phases or times for the maximum

T(p) of the QBO or IA terms exhibit a slow advance in their cycles as they proceed toward lower altitudes. This coherent character for the phase of T(p) is in accord with the rate of descent for the alternating mean QBO easterlies and westerlies of the middle atmosphere. It is another measure of the good quality of the HALOE T(p) data for these analyses.

c. Solar Cycle or SC-like Term

Remsberg and Deaver [2005, their Figure 6] showed a model fit to their time series for 40N and 0.03 hPa (or near 70 km). They found a significant QBO-like term with a period of 903 days and a solar cycle term. Figure 9 shows the results of the re-analysis of the extended time series for that latitude and level. The model includes a significant QBO term with a period of 853 days, plus the prescribed, periodic 4015-dy or 11-yr SC term. The effect of both of those terms is clearly evident in the data and the model in Figure 9. A linear trend term has also emerged and is included; it has a rate of cooling of -2.3 K/decade and is 99.8% significant (see following subsection, too).

Remsberg and Deaver [2005] did not find a highly significant trend at 40N and 0.03 hPa, most likely because of their incorrect method of accounting for the autoregressive effects for all the terms of their time series. Their SC-like term had amplitude 0.8 K and its maximum occurred 2.2 yr after January 1, 1991. The same SC-like term from the re-analysis has amplitude 1.0 K (99.7% significant) and its maximum occurs 1.3 yr after January, 1991. It is in-phase with that of the more traditional solar flux proxies. The

shift of the phase of the re-analyzed SC term to one year earlier is primarily a result of resolving the concurrent trend term and including it in the time series model.

Table 10 displays the amplitude of the significant SC-like terms from the re-analyses. Note that these amplitudes are equivalent to one-half the 'solar max minus solar min' values reported by most analysts and modelers. SC-like terms are not reported for HALOE, if their significance is less than 85%. That is why no corresponding contour plot is provided for the amplitudes of these terms, as one might wish for purposes of comparisons with results from numerical models. The largest SC-like temperature responses are found at middle latitudes of the upper mesosphere. Where significant, the responses in the middle mesosphere are only half as strong.

Table 11 contains the phase of the maximum T(p) of the SC-like terms, as measured in years past January 1, 1991. Because the approach for the analyses of the SC term herein was merely to find the best fit for a term of 11-yr period, it was expected that there would not be an exact match to the time of the rather broad maximum from the traditional solar flux proxies. That is why the present results for the SC-like term are considered somewhat exploratory, rather than definitive. Still, its phases are almost always within ±2 yrs of January 1991. Exceptions occur in the upper mesosphere at 60S and in the lower mesosphere and upper stratosphere at 60N. Those anomalies may be due to the high latitudes not being sampled as well, such that the rather large amplitudes of its seasonal cycles are not accounted for accurately. A somewhat out-of-phase relationship at high latitudes may also be an indication of a dynamically-induced, decadal-scale term

in the T(p) time series, perhaps related indirectly to the solar cycle. It is also noted that there is a somewhat out-of-phase relationship for the SC-like term at the 3 hPa level. The HALOE V19 retrievals of T(p) rely on the NOAA CPC analyses at 5 hPa and below, and there was a shift to slightly lower values in 2001 and thereafter for the CPC dataset due to a change in their analysis procedures. The effect of that shift was illustrated in a plot of the T(p) time series at 10N, 5 hPa in *Remsberg and Deaver* [2005]. It is likely that some effect of that shift remains in the time series of HALOE T(p) even at 3 hPa.

In order to illustrate the direct SC-like variations of T(p) with altitude and latitude, some qualitative profiles are provided in Figure 10. First, the amplitudes of the SC-like terms in Table 10 were adjusted for the fact that the fitted SC-like terms were not exactly in-phase (coinciding with January 1991). Those adjustments were made by simply multiplying the amplitude by the factor, cos [2πp/11], where the phase p (in yrs) was taken from Table 11 and divided by the presumed 11-yr SC period. The adjusted amplitudes were averaged within the latitude ranges of 30-60S, 20S-20N, and 30-60N at each pressure level, with only those terms having phases in Table 11 within ±2 yrs of January 1991 being retained. The adjusted amplitudes of the terms that met that phase criterion were then multiplied by 2 to give an estimate of the observed 'max minus min' values for comparisons with the responses of the direct SC forcings that have been published by others from analyses of their datasets and/or from their model studies. Finally, the profiles for the 30-60 latitude regions of the NH and SH were averaged to obtain a single response profile for the middle latitudes. Those average middle and low latitude profiles are shown in Figure 10. They have 'max minus min' values of about 1.0

K near the stratopause, of between 0.7-1.5 K in the lower mesosphere, and then increasing to about 2.0-2.5 K in the upper mesosphere. The estimated, direct SC response for the low latitude zone is weaker throughout the mesosphere. It is also important to remember that the average profiles for both latitude zones are likely upper limits. That caveat is particularly true at levels of the middle mesosphere at the low latitudes and at the middle latitudes of the NH, where often no significant SC-like term was resolved from the HALOE time series (see Table 10).

The qualitative HALOE results of Figure 10 are in good accord with the findings from the modeling studies of *Garcia et al.* [1984], *Huang and Brasseur* [1993], and *McCormick and Hood* [1996], among others. The HALOE adjusted, zonal-mean SC 'max minus min' differences of 1.4 to 3.2 K for the upper mesosphere at 40N-50N are also in reasonable agreement with the combined, 'summer plus winter', results from the ground-based, Rayleigh lidar measurements at 44N [*Keckhut et al.,* 2005, their Figure 3]. The T(p) responses from the models are fairly uniform with latitude. Conversely, the SC-like amplitudes from HALOE for the upper mesosphere are larger for middle latitudes of the NH than for the SH or the low latitudes (see Table 10), perhaps due to the effects of breaking planetary waves that tend to be more prevalent for NH winter and which may vary somewhat with the solar cycle. The interfering effects of the tides and gravity waves may also be imparting a larger, noise-like structure onto the HALOE time series data at lower latitudes, leading to difficulties for resolving its smaller amplitude seasonal and longer-period terms.

Model studies indicate a significant, secondary maximum for the SC response near the tropical stratopause. The model 'max minus min' results have upper limits that vary from 2.2 K [*Garcia et al.,* 1984; *McCormick and Hood*, 1996] to 1.4 K [*Huang and Brasseur,* 1993] and to 1.1 K [*Matthes et al.,* 2004]. The upper limit from the HALOE re-analysis is in the range of 0.6 to 1.4 K or at the low end of the model results. The HALOE values in this region are also somewhat smaller than reported from the NCEP re-analyses [*Hood*, 2004] and from the ERA-40 dataset [*Crooks and Gray*, 2005], though they agree fairly well with the SC analyses from the SSU satellite radiances [*Scaife et al.,* 2000]. However, those NCEP/ERA-40/SSU results were based on datasets that extended from 1979 to either 1997 or 2001 and are not strictly representative of the 1991-2005 period of HALOE. To first order though, such a mismatch in the respective time spans of the datasets should not be a problem for a truly periodic SC term, unless there are other underlying, long-period and/or trend terms that have not been accounted for properly. The weaker SC-like response from HALOE near the tropical stratosphere versus the model values may be an indication of the interfering influences of wave activity that are known to vary according to the easterly versus the westerly phases of the QBO cycle [e.g., *Salby and Callaghan*, 2006].

d. Linear Trend Term

Table 12 shows that there are significant cooling trends for the HALOE time series at a number of latitudes and pressure levels. Those effects are largest and most easily resolved for middle latitudes of the middle to upper mesosphere, although they are somewhat larger than predicted (see below). In order to obtain trend terms for more of

the latitudes and pressure levels of Table 12, the lower acceptance limit for the significance of that term was reduced to 76%. Even so, almost all of the terms in Table 12 have a level of significance of at least 90%. Several aspects of the results in Table 12 are noteworthy, but their causes have not been evaluated fully. First, while significant trend terms have emerged at most all the levels of 60S, there are none at 60N. Second, the magnitudes of the trend terms are clearly decreasing at the uppermost levels of the mesosphere at NH middle latitudes, and trend terms did not emerge at those levels at lower latitudes (except at the Equator). Finally, the cooling trends below the stratopause at low latitudes appear to be increasing with decreasing altitude, perhaps due to associated effects of the trends in ozone during this 14-yr period [*Shine et al.*, 2003].

Because the determination of a trend term is subject to small biases for the time series, it may be unwise to assume that all of the entries of Table 12 have equal certainty. As noted earlier, the sampling for HALOE became less frequent in the latter half of the UARS mission for the latitudes of 40-60 degrees. On the other hand, the latitudes equatorward of about 35 degrees were sampled much more evenly with season and throughout the mission, although significant trend terms did not emerge at most levels for the lowest latitudes. Figure 11 is an assembly of the overall results from Table 12. First, the averages of the trends are shown for the two middle latitude ranges of 20-60S and 20-50N. Those NH results only extend down to the 0.3 hPa level, but in the middle mesosphere they agree well with those of the SH middle latitudes. At higher altitudes the NH trend is about twice that of the SH. When the trend terms for the latitudes of 20 and 30 degrees of each hemisphere are considered, they agree much more closely with each

other. Those subtropical trends have been averaged and are shown by the solid curve of Figure 12. Trends from the solid curve are of order -0.5 K/decade in the uppermost stratosphere and the lower mesosphere, increasing to about -1.0 K/decade in the upper mesosphere. It is the solid curve that may be the most representative of the radiative cooling effects due to the steady increases of CO2. That range of values from HALOE agrees well with the trends of -0.6 K/decade just below the stratopause and of -0.8 K/decade in the lower mesosphere that were obtained for the simulated responses of temperature versus pressure due to the observed increases in CO2 from 1955 to 1995 (from Figure 2 in *Akmaev and Fomichev* [2000]). The larger HALOE trends of the upper mesosphere at NH middle latitudes may be because of added effects for the net circulation of the mesosphere due to long-term changes in the planetary wave forcing from below.

4. Summary findings

A re-analysis was conducted of time series of zonal averages of the temperature versus pressure profile data (or T(p)) provided by the 14+ years of HALOE measurements from the UARS satellite. The findings from the re-analyses are now clearer and more significant because of a proper accounting for the effects of autoregression for the adjacent points of the time series. One can generate definitive monthly or seasonal climatologies of T(p) for the middle atmosphere levels from 3 hPa to 0.007 hPa and for the period 1991-2005 based on the seasonal and annual mean terms of Tables 3-7 herein; the effects of the interannual and solar cycle variations are already removed for those tables. In addition, the amplitudes, phases, and periods of the primary interannual (IA) or QBO-like terms are also considered as definitive (where they emerged), because 6 complete cycles occurred in this 14-year period. The amplitudes of those QBO-like terms vary from 0.3 and 1.9 K.

Beig et al. [2003] reported recently on the large amount of uncertainty for the longer-term changes in middle atmosphere temperature. Results from the analysis of a 9.5-yr time series of HALOE data in *Remsberg et al.* [2002a] were contributed to that review paper, but those authors were generally unable to find significant fits for the solar cycle or trend terms because of their incorrect treatment of the effects of autoregression. Their dataset was extended by nearly 5 more years and re-analyzed properly in the present study; significant terms have emerged at many more latitudes and levels. These re-analyses for

the 11-yr solar cycle or SC-like terms and the linear trend terms are considered somewhat exploratory in nature, especially because only one complete solar cycle has been spanned. Nevertheless, the results for these terms are very reasonable and coherent with latitude and pressure-altitude. The prescribed 11-yr, SC-like terms are generally in phase with the standard proxies for the direct solar flux. After making adjustments for any slight mismatches in the phases, the SC terms lead to 'max minus min' values for T(p) of order 1 K in the upper stratosphere to the middle mesosphere, and then increasing to about 2.0 to 2.5 K in the upper mesosphere. Average profiles of the SC response are larger for the middle latitudes than for the low latitudes. Both of these qualitative variations with pressure-altitude and with latitude tend to agree with the SC responses that have been obtained with models. It is stressed though that the actual nature of the SC-like terms from the HALOE re-analyses are the amplitudes of Table 10 and the phases of Table 11.

Significant, linear trend (cooling) terms were found at many latitudes and pressure-altitudes. Their magnitudes are generally larger than predicted from models of the radiative effects due to the steady increases of CO2 in the middle atmosphere, especially at the middle latitudes. There may be biases in the derived trends poleward of about 35 degrees latitude, due to a seasonal non-uniformity for the HALOE sampling over the UARS mission. There may also be contributions to those trends from dynamical effects. A sporadic or incomplete sampling is not a problem for the latitudes of 20 and 30 degrees of both hemispheres, however; the trend terms at those latitudes vary from -0.5 to -1.0 K/decade and are in good agreement with the model estimates of *Akmaev and Fomichev* [2000]. Furthermore, calibration measurements were taken over the course of

the HALOE mission and analyzed recently to determine whether there might have been some long-term degradation of the HALOE instrument that is affecting the results of these re-analyses. No problems have been found that would affect the trends from T(p) [*Gordley et al.*, 2006]. Thus, it is tentatively concluded that the present findings about the longer-term changes of T(p) in the middle atmosphere are also appropriate values for comparison with models.

Acknowledgments. The author embarked on this analysis as a result of his invitation to participate in a Workshop hosted by K. Kodera at the 2004 Fall AGU Meeting. He is most grateful for the very helpful comments of an anonymous reviewer of his earlier JGR submitted manuscript regarding the erroneous assessment of the effects of autocorrelation in his previously published studies of the temperature and ozone data from HALOE. He has also benefited from his interactions with Lon Hood and Boris Soukharev, who have undertaken similar studies of the SC responses in ozone from SBUV and HALOE and in temperature from the NCEP reanalysis datasets. The author also appreciates having discussions of his findings with Elizabeth Weatherhead and with his colleague, Murali Natarajan. Support for this work was provided by the UARS Program Office at NASA Headquarters and the UARS Project Office at NASA/GSFC.

References

Akmaev, R. A., and V. I. Fomichev (2000), A model estimate of cooling in the mesosphere and lower thermosphere due to the CO2 increase over the last 3-4 decades, *Geophys. Res. Lett., 27,* 2113-2116.

Barnett, J. J., M. Corney, and K. Labitzke (1985), Annual and semiannual cycles based on the middle atmosphere reference model in Section 2.2, in Handbook for Middle Atmosphere Program (MAP), vol. 16, K. Labitzke, J. J. Barnett, and B. Edwards, Eds., SCOSTEP Secretariat, U. of Illinois, Urbana, IL, 175-180.

Beig, G., P. Keckhut, R. P. Lowe, R. G. Roble, M. G. Mlynczak, J. Scheer, V. I. Fomichev, D. Offermann, W. J. R. French, M. G. Shepherd, A. I. Semenov, E. E. Remsberg, C-Y. She, F. J. Lubken, J. Bremer, B. R. Clemesha, J. Stegman, F. Sigernes, S. Fadnavis (2003), Review of mesospheric temperature trends, *Rev. Geophys., 41,* doi:10.1029/2002RG000121.

Crooks, S. A., and L. J. Gray (2005), Characterization of the 11-year solar signal using a multiple regression analysis of the ERA-40 dataset, *J. Climate, 18*, 996-1015.

Dudhia, A., S. E. Smith, A. R. Wood, and F. W. Taylor (1993), Diurnal and semi-diurnal temperature variability of the middle atmosphere, as observed by ISAMS, *Geophys. Res. Lett., 20,* 1251-1254.

Garcia, R. R., S. Solomon, R. G. Roble, and D. W. Rusch (1984), A numerical response of the middle atmosphere to the 11-year solar cycle, *Planet. Space Sci., 32*, 411-423.

Gordley, L. L., B. Magill, E. Thompson, M. McHugh, E. Remsberg, and J. Russell III (2006), Accuracy of atmospheric trends inferred from HALOE data, *for submission to J. Geophys. Res.-Atmos.*

Hervig, M., and D. Siskind (2005), Decadal and inter-hemispheric variability in polar mesospheric clouds, water vapor, and temperature, J. *Atmos. Solar Terr. Phys.,* doi:10.1016/j.jastp.2005.08.010.

Hood, L. (2004), Effects of solar uv variability on the stratosphere, in *Solar Variability and its Effects on Climate*, Geophysical Monograph 141, AGU, 283-303.

Huang, T. Y. W., and G. P. Brasseur (1993), Effect of long-term solar variability in a two-dimensional interactive model of the middle atmosphere, *J. Geophys. Res., 98*, 20,413-20,427.

Keckhut, P., C. Cagnazzo, M.-L. Chanin, C. Claud, and A. Hauchecorne (2005), The 11-year solar-cycle effects on the temperature in the upper-stratosphere and mesosphere: Part I—Assessment of observations, *J. Atmos. Solar Terr. Phys.,* doi:10.1016/j.jastp.2005.01.008.

Leblanc, T., and, A. Hauchecorne (1997), Recent observations of mesospheric temperature inversions, *J. Geophys. Res., 102*, 19,471-19,482.

Matthes, K., U. Langematz, L. L. Gray, K. Kodera, and K. Labitzke (2004), Improved 11-solar signal in the Freie Universitat Berlin Climate Middle Atmosphere Model (FUB-CMAM), *J. Geophys. Res., 109*, D06101, doi:10.1029/2003JD004012.

McCormack, J. P., and L. L. Hood (1996), Apparent solar cycle variations of upper stratospheric ozone and temperature: latitude and seasonal dependences, *J. Geophys. Res., 101*, 20,933-20,944.

McHugh, M., M. Hervig, B. Magill, E. Thompson, E. Remsberg, J. Wrotny, and J. M. Russell III (2003), Improved mesospheric temperature, water vapor, and polar mesospheric cloud extinctions from HALOE, *Geophys. Res. Lett., 30*, doi:10.1029/2002GL016859.

Remsberg, E. E., P. P. Bhatt, and L. E. Deaver (2002a), Seasonal and longer-term variations in middle atmosphere temperature from HALOE on UARS, *J. Geophys. Res., 107*, doi:10.1029/2001JD001366.

Remsberg, E. E., et al. (2002b), An assessment of the quality of halogen occultation experiment temperature profiles in the mesosphere based on comparisons with Rayleigh

backscatter lidar and inflatable falling sphere measurements, *J. Geophys. Res., 107*, doi:10.1029/2001JD001521.

Remsberg, E. E., and L. E. Deaver (2005), Interannual, solar cycle, and trend terms in middle atmospheric temperature time series from HALOE, *J. Geophys. Res., 110*, D06106, doi:10.1029/2004JD004905.

Salby, M. L., and P. F. Callaghan (2006), Relationship of the quasi-biennial oscillation to the stratospheric signature of the solar cycle, *J. Geophys. Res., 111*, D06110, doi:10.1029/2005JD006012.

Scaife, A. A., J. Austin, N. Butchart, S. Pawson, M. Keil, J. Nash, and I. N. James, Seasonal and interannual variability of the stratosphere diagnosed from UKMO TOVS analyses (2000), *Quart. J. Roy. Meteorol. Soc., 126*, 2585-2604.

Shine, K. P., et al. (2003), A comparison of model-simulated trends in stratospheric temperatures, *Quart. J. Roy. Meteorol. Soc., 129*, 1565-1588.

Siskind, D. E., S. D. Eckermann, J. P. McCormack, M. J. Alexander, and J. T. Bacmeister (2003), Hemispheric differences in the temperature of the summertime stratosphere and mesosphere, *J. Geophys. Res., 108*, doi:10.1029/2002JD002095.

Tiao, G. C., G. C. Reinsel, D. Xu, J. H. Pedrick, X. Zhu, A. J. Miller, J. J. DeLuisi, C. L. Mateer, and D. J. Wuebbles (1990), Effects of autocorrelation and temporal sampling schemes on estimates of trend and spatial correlation, *J. Geophys. Res., 95*, 20,507-20,517.

Figure 1. Time series of zonal average SR (open circles) and SS (solid circles) temperatures (K) from HALOE measurements at 30ºN and the 0.02-hPa level (near 74 km) of the mesosphere. Points have been adjusted to first order for the average diurnal difference at SR versus SS. Terms for the multiple linear regression (MLR) model fit are listed at the lower left (see text). The oscillating curve is the fit for the complete MLR model, while the straight line is the fit based on the constant and linear trend terms.

Figure 2. Contour plot of the autocorrelation coefficients at lag-1 (or AR1) from the analyses of the HALOE temperature time series in terms of latitude versus pressure-altitude. Altitude scale on the right is approximate.

Figure 3. Contour plot of the zonal average temperature amplitude (K) for the annual oscillation (AO) term of the MLR model. Contour interval is 2 K.

Figure 4. Contour plot of the phase (month of the year) for the AO temperature maximum (see text). Contour interval is 2 months.

Figure 5. As in Figure 3, but for the amplitude of the semi-annual oscillation (SAO) term. Contour interval is 1 K.

Figure 6. Contour plot of the annual-mean, zonal-average temperature distribution from the MLR model. Contour interval is 5 K.

Figure 7. As in Figure 1, but at 60ºN and the 0.007-hPa level (near 80 km). Note the apparent effects of the several day-per-year precession for the springtime samples for SR from mid 1996 through 2001.

Figure 8. As in Figure 1, but at 20ºS and the 3-hPa level of the upper stratosphere. There are two separate and significant interannual terms for its MLR model, and they have average periods of 853 and 640 days, respectively.

Figure 9. As in Figure 1, but at 40ºN and the 0.03-hPa level (near 70 km).

Figure 10. Average profiles of the adjusted, 'max minus min' differences of the T(p) response of the 11-yr solar cycle (or SC-like) term of the MLR model. The dashed profile is the average response for the middle latitudes of the southern plus northern hemispheres, while the solid profile is the average for 20S-20N.

Figure 11. Average profiles of the linear trend terms (in K/decade) for the three latitude zones of 20-60S, of 20-50N, and then of the subtropics (20-30º) from both hemispheres.

Table 1—Absolute Value of Autocorrelation Coefficient

P(hPa)	60S	50S	40S	30S	20S	10S	Eq	10N	20N	30N	40N	50N	60N
0.007	0.36	0.23	0.36	0.04	0.05	0.20	0.08	0.13	0.12	0.12	0.01	0.19	0.14
0.010	0.39	0.25	0.09	0.02	0.01	0.17	0.19	0.08	0.03	0.24	0.13	0.19	0.15
0.015	0.36	0.31	0.22	0.08	0.06	0.07	0.24	0.10	0.02	0.30	0.22	0.27	0.26
0.020	0.33	0.32	0.25	0.19	0.10	0.05	0.19	0.07	0.08	0.34	0.22	0.27	0.27
0.030	0.36	0.29	0.22	0.18	0.08	0.00	0.18	0.05	0.02	0.23	0.28	0.33	0.36
0.050	0.43	0.38	0.26	0.14	0.06	0.11	0.15	0.06	0.05	0.19	0.34	0.41	0.40
0.070	0.48	0.45	0.30	0.17	0.02	0.07	0.18	0.16	0.00	0.22	0.40	0.42	0.38
0.100	0.52	0.46	0.30	0.20	0.08	0.04	0.15	0.03	0.05	0.24	0.38	0.40	0.37
0.150	0.52	0.49	0.36	0.21	0.20	0.04	0.16	0.12	0.12	0.20	0.28	0.37	0.46
0.200	0.45	0.50	0.36	0.22	0.30	0.03	0.18	0.01	0.19	0.14	0.28	0.36	0.49
0.300	0.45	0.43	0.36	0.25	0.31	0.20	0.19	0.10	0.21	0.16	0.34	0.32	0.41
0.500	0.43	0.43	0.36	0.30	0.21	0.04	0.28	0.06	0.23	0.29	0.36	0.36	0.35
0.700	0.33	0.37	0.30	0.25	0.18	0.13	0.29	0.13	0.14	0.31	0.40	0.42	0.32
1.000	0.25	0.33	0.30	0.22	0.27	0.23	0.30	0.22	0.25	0.29	0.43	0.40	0.25
1.500	0.33	0.31	0.35	0.22	0.16	0.12	0.19	0.12	0.26	0.19	0.38	0.36	0.21
2.000	0.35	0.33	0.36	0.24	0.26	0.28	0.30	0.26	0.31	0.26	0.40	0.34	0.23
3.000	0.36	0.38	0.39	0.46	0.39	0.58	0.57	0.50	0.32	0.56	0.46	0.32	0.35

Table 2—HALOE Sunset Minus Sunrise Temperature (K)

P(hPa)	60S	50S	40S	30S	20S	10S	Eq	10N	20N	30N	40N	50N	60N
0.007	0.6	-0.6	0.6	3.0	1.7	-3.2	-6.1	-3.4	1.7	2.2	2.5	-0.5	-0.7
0.010	1.1	0.3	3.9	4.5	1.4	-5.2	-8.3	-5.9	1.5	3.4	3.6	0.2	-0.1
0.015	0.6	2.5	3.3	3.9	-0.0	-5.3	-7.8	-5.4	0.3	2.8	3.1	-0.1	-0.5
0.020	-0.3	-1.0	2.3	2.6	-0.6	-3.7	-5.3	-4.5	-0.3	1.9	2.1	-0.8	-1.1
0.030	-1.4	-2.5	0.5	0.5	-0.1	-0.1	-0.5	-1.8	-0.8	0.5	0.2	0.0	-1.8
0.050	-1.7	-4.1	-1.6	-1.8	1.1	3.7	4.2	1.7	0.3	-1.1	-1.9	-2.2	-1.8
0.070	-1.1	-4.3	-2.6	-2.4	1.6	5.0	6.0	3.7	1.0	-1.9	-2.8	-1.9	-1.8
0.100	-0.5	-4.0	-3.2	-2.3	1.7	5.3	7.0	5.1	1.4	-2.2	-2.7	-1.5	-1.3
0.150	0.4	-3.2	-2.7	-1.3	1.8	4.9	6.9	5.4	1.6	-1.5	-1.6	-0.4	-0.5
0.200	1.0	-1.9	-1.8	-0.2	1.7	4.3	6.5	5.0	1.3	-0.4	-0.4	0.7	0.1
0.300	1.9	0.1	-0.2	1.3	2.0	3.4	5.4	3.9	1.6	1.4	1.3	2.1	1.4
0.500	3.1	2.9	1.5	2.8	2.6	2.3	3.0	2.3	2.5	3.3	3.2	3.6	2.8
0.700	3.7	4.3	2.6	3.4	2.9	1.4	0.7	1.6	3.3	3.9	3.9	4.2	3.5
1.000	3.9	5.5	3.4	3.6	2.8	0.8	-0.7	1.1	3.5	4.0	4.2	4.6	3.8
1.500	3.6	5.8	3.3	3.0	1.7	0.2	-0.7	0.6	2.2	3.5	3.5	4.5	3.6
2.000	3.1	5.0	2.3	2.3	0.8	0.1	-0.4	0.0	1.2	2.7	2.5	3.5	3.1
3.000	2.0	3.6	0.7	1.1	0.5	0.2	0.0	-0.0	0.6	1.5	0.9	2.0	1.6

Table 3—Amplitude of Annual Cycle (K)

P(hPa)	60S	50S	40S	30S	20S	10S	Eq	10N	20N	30N	40N	50N	60N
0.007	23.6	14.9	23.8	5.0	0.8	1.2	1.4	0.9	4.5	8.6	12.6	17.6	20.6
0.010	22.1	14.2	9.4	3.9	---	1.4	1.5	1.0	4.1	8.3	12.6	16.8	19.5
0.015	20.6	13.8	8.3	2.1	2.3	1.4	2.1	1.6	3.5	7.5	11.5	15.6	18.2
0.020	19.8	13.8	8.0	1.0	1.2	1.6	2.4	2.1	3.4	6.9	10.6	14.8	17.4
0.030	18.1	13.2	7.5	---	1.6	1.6	2.1	2.5	3.6	6.3	9.2	13.2	16.0
0.050	12.1	10.6	6.1	1.4	2.1	1.9	1.9	3.1	3.5	4.3	6.6	9.4	11.9
0.070	6.4	7.7	4.3	1.5	2.2	2.3	2.5	3.4	3.1	2.8	4.4	6.1	7.5
0.100	1.2	4.3	2.0	1.5	2.1	2.7	3.0	3.5	2.5	1.8	1.9	2.9	3.0
0.150	5.7	0.9	1.3	1.8	2.0	2.6	3.2	3.3	1.9	0.9	---	2.5	2.7
0.200	10.2	3.1	3.5	1.9	1.8	2.4	3.0	2.9	1.4	0.6	2.3	4.3	5.7
0.300	14.6	6.9	6.0	2.4	1.6	2.3	2.7	2.3	1.0	1.0	4.1	6.9	9.6
0.500	16.9	11.1	8.4	3.6	1.3	1.9	2.4	2.2	0.7	1.7	5.6	9.3	13.8
0.700	17.0	13.4	9.6	4.4	1.3	1.5	2.4	2.0	0.8	1.8	6.1	10.5	16.6
1.000	18.5	15.5	10.8	5.0	1.5	1.3	2.2	1.6	0.9	1.9	6.6	11.7	18.9
1.500	20.4	17.5	12.3	6.3	2.3	1.0	1.3	0.9	1.0	2.8	7.5	12.8	19.8
2.000	20.2	18.1	12.9	7.5	2.7	0.6	1.3	1.2	1.6	3.7	8.1	12.9	19.1
3.000	19.5	17.2	12.1	6.9	2.5	0.6	1.1	0.9	1.6	3.7	7.8	12.2	17.5

Table 4—Day of Year for the Maximum of the Annual Cycle

P(hPa)	60S	50S	40S	30S	20S	10S	Eq	10N	20N	30N	40N	50N	60N
0.007	176	179	176	183	253	329	361	345	4	2	2	362	364
0.010	177	180	178	185	---	325	339	328	6	4	5	365	2
0.015	178	181	178	190	348	320	326	324	358	11	8	4	6
0.020	179	182	177	179	356	300	326	328	10	17	10	6	7
0.030	177	182	174	---	363	327	326	344	14	19	10	8	8
0.050	177	184	175	73	9	9	361	1	11	8	5	10	9
0.070	179	186	175	74	19	21	11	4	3	355	2	18	12
0.100	214	190	177	59	24	19	12	4	361	327	3	42	32
0.150	341	270	348	27	25	15	9	5	358	289	---	129	141
0.200	345	338	353	12	24	15	11	10	362	237	167	152	158
0.300	346	351	354	362	17	17	15	18	9	174	168	159	162
0.500	345	354	355	352	2	24	31	31	33	163	163	162	165
0.700	343	356	356	349	365	30	37	39	45	152	160	163	166
1.000	344	356	355	348	1	43	48	43	39	135	157	164	168
1.500	344	357	357	351	357	57	83	89	94	138	156	166	169
2.000	344	357	358	352	349	71	127	125	119	141	156	167	170
3.000	344	358	358	354	349	49	127	112	111	133	154	168	171

Table 5—Amplitude of SemiAnnual Cycle (K)

P(hPa)	60S	50S	40S	30S	20S	10S	Eq	10N	20N	30N	40N	50N	60N
0.007	5.5	4.8	5.4	0.6	1.0	1.0	1.8	1.1	0.6	2.0	2.5	4.2	7.4
0.010	5.2	4.7	2.0	1.4	1.6	2.4	3.0	2.2	2.0	2.8	2.6	4.2	7.7
0.015	4.8	4.8	2.4	2.1	2.7	4.2	4.5	4.4	3.3	3.5	3.1	4.6	8.0
0.020	4.4	4.7	2.5	2.5	3.6	5.5	5.9	5.5	3.9	3.8	3.4	5.1	7.6
0.030	4.0	5.1	2.9	2.0	3.7	6.1	7.0	6.1	4.1	3.7	3.6	5.9	6.5
0.050	3.7	5.8	4.1	2.0	2.4	4.9	6.0	5.5	3.3	2.5	4.2	6.7	4.3
0.070	3.3	6.0	4.6	2.2	1.5	3.9	4.7	4.1	2.3	1.6	4.7	6.9	3.2
0.100	2.9	5.9	4.7	2.6	1.1	3.1	3.5	2.9	1.6	2.0	5.1	6.8	2.7
0.150	1.8	5.7	4.3	2.9	1.5	2.2	2.1	2.0	1.3	2.5	5.2	6.1	2.1
0.200	1.3	5.3	3.7	2.7	1.8	1.6	1.4	1.7	1.5	2.6	4.7	5.2	1.6
0.300	1.9	4.4	2.8	2.3	1.8	1.1	1.1	1.6	1.6	2.5	3.8	4.2	0.8
0.500	2.3	3.3	1.7	1.7	1.3	1.0	1.0	1.3	1.7	2.4	2.8	2.6	---
0.700	2.5	2.9	0.9	1.4	1.1	1.5	1.8	1.7	1.5	1.9	2.0	2.0	0.5
1.000	2.8	2.9	---	0.9	0.9	2.4	3.2	2.4	1.5	1.0	1.0	1.9	0.8
1.500	2.9	3.2	1.4	0.7	0.7	2.3	3.2	2.6	1.0	0.5	0.7	2.7	0.7
2.000	3.0	3.3	1.8	0.8	0.8	2.5	3.5	2.7	0.9	0.5	1.0	3.3	1.3
3.000	2.8	3.0	2.0	0.8	1.1	2.8	3.6	2.8	1.3	---	0.9	3.3	1.7

Table 6—Day of Year for the Maximum of the First SemiAnnual Cycle

P(hPa)	60S	50S	40S	30S	20S	10S	Eq	10N	20N	30N	40N	50N	60N
0.007	102	86	103	21	1	169	157	151	1	12	37	71	90
0.010	105	88	69	33	9	175	167	173	4	21	43	76	95
0.015	110	94	75	40	15	182	179	182	8	27	50	81	99
0.020	117	101	84	49	18	5	4	5	14	35	57	86	103
0.030	132	114	99	63	22	15	15	15	21	44	72	93	109
0.050	147	130	117	95	28	27	28	26	29	58	92	104	123
0.070	156	139	124	110	33	34	36	32	31	79	102	111	132
0.100	166	149	133	118	54	44	43	39	34	101	112	118	142
0.150	182	160	138	119	76	54	44	42	45	106	114	123	152
0.200	24	167	144	119	78	55	42	42	53	107	118	130	158
0.300	46	180	150	121	85	56	37	43	65	107	124	135	163
0.500	44	13	162	134	99	64	52	53	82	112	131	146	---
0.700	33	26	173	144	110	75	70	71	98	119	137	158	69
1.000	33	37	---	161	112	83	82	85	109	132	140	177	66
1.500	35	41	39	10	119	99	97	99	114	172	5	7	39
2.000	32	41	46	25	121	108	106	107	116	3	14	12	15
3.000	37	45	54	50	108	110	110	111	115	---	14	14	16

Table 7—Annual Average Temperature Distribution from HALOE

P(hPa)	60S	50S	40S	30S	20S	10S	Eq	10N	20N	30N	40N	50N	60N
0.007	194.1	193.2	194.0	194.9	193.2	192.7	193.5	191.0	190.7	192.3	192.3	191.1	188.3
0.010	197.1	196.2	197.1	195.9	194.1	193.8	194.4	192.5	192.3	193.7	194.9	194.2	191.0
0.015	200.1	199.7	199.7	196.8	195.0	194.4	194.8	193.6	193.8	196.3	198.2	198.2	194.1
0.020	203.1	202.0	202.1	198.0	196.7	195.0	194.1	194.6	195.2	198.6	200.8	201.1	197.4
0.030	209.3	207.2	206.4	203.0	200.5	197.9	196.3	197.7	200.0	203.4	205.4	205.9	204.1
0.050	218.8	216.4	214.3	212.5	210.7	206.9	205.0	207.0	210.0	212.6	213.6	214.1	215.9
0.070	225.6	223.4	221.0	219.7	218.8	215.6	214.2	215.4	218.1	220.0	220.1	221.2	224.2
0.100	233.8	230.9	228.5	227.3	227.1	225.7	225.3	225.7	226.7	226.8	227.4	228.8	232.8
0.150	241.4	238.3	236.4	235.3	235.7	236.8	237.4	237.4	237.1	235.6	234.9	237.2	241.6
0.200	245.8	243.6	241.7	240.6	242.0	243.8	244.9	244.5	243.4	241.3	241.2	243.6	246.9
0.300	251.7	250.1	248.2	248.0	249.9	252.3	253.5	252.8	250.9	248.4	248.5	250.8	252.9
0.500	257.9	256.2	254.7	256.0	258.6	260.9	261.7	260.9	258.3	256.0	255.9	257.5	258.1
0.700	261.7	258.7	258.3	260.3	262.9	264.7	265.8	264.3	262.2	260.3	259.6	260.4	259.6
1.000	262.1	259.4	259.8	262.8	265.0	265.6	266.3	265.8	264.3	262.6	261.7	261.3	259.1
1.500	259.3	256.8	258.1	261.2	263.0	263.5	263.8	264.0	262.6	261.6	260.4	259.0	255.8
2.000	255.9	253.1	254.4	257.7	259.3	259.9	260.0	260.0	259.4	258.9	257.1	255.2	252.0
3.000	249.0	246.9	247.9	250.4	251.8	252.6	252.5	252.5	252.2	251.7	249.9	248.0	245.0

Table 8—Annual Mean SH minus NH Temperature Difference (K) by Latitude Zone

P(hPa)	60	50	40	30	20	10
0.007	5.8	2.1	1.7	2.6	0.9	2.0
0.010	6.1	2.0	2.9	2.2	1.8	1.5
0.015	6.0	1.5	1.5	0.5	1.2	0.8
0.020	5.7	0.9	1.3	-0.6	1.5	0.4
0.030	5.2	1.3	1.0	-0.4	0.5	0.2
0.050	2.9	2.3	0.7	-0.1	0.7	-0.1
0.070	1.4	2.2	1.0	-0.3	0.7	0.2
0.100	1.0	2.1	1.1	0.5	0.4	-1.0
0.150	-0.2	1.1	1.5	-0.3	-1.4	-0.3
0.200	-1.1	0.0	0.5	-0.7	-1.4	0.5
0.300	-1.2	-0.7	-0.3	-0.4	-1.0	1.4
0.500	-0.2	-1.3	-1.2	0.0	0.3	1.6
0.700	2.1	-1.7	-1.3	0.0	0.7	1.5
1.000	3.0	-1.9	-1.9	0.2	0.7	1.3
1.500	3.5	-2.2	-2.3	-0.4	0.4	0.9
2.000	2.1	-2.1	-2.7	-1.2	-0.1	0.5
3.000	4.0	-1.1	-2.0	-1.3	-0.4	0.4

Table 9—Amplitude of Interannual or QBO-Like Term (K)

P(hPa)	60S	50S	40S	30S	20S	10S	Eq	10N	20N	30N	40N	50N	60N
0.007	1.0	---	0.8	---	---	---	0.7*	---	1.2*	0.5	0.7*	0.6	---
0.010	0.7	---	---	---	---	---	1.2*	---	---	0.7	1.0	0.7	---
0.015	---	0.7	0.5	---	---	---	1.8*	1.1*	---	0.8	1.3	1.0	0.8
0.020	---	---	1.0	---	---	---	1.7*	---	---	0.8	1.6	1.3	1.1
0.030	---	1.1	1.6	---	---	---	---	---	---	0.8	1.7	1.6	1.1*
0.050	---	1.1	1.5	---	---	---	---	---	---	0.8	1.9	1.7	1.2
0.070	---	1.0	1.4	---	---	---	---	---	---	1.0	1.6	1.4	0.8
0.100	---	0.7	1.2	---	---	---	---	---	---	1.0	1.0	1.0	---
0.150	---	0.9	1.0	---	---	---	---	---	---	0.5*	---	0.5	---
0.200	0.7*	1.3	1.1	---	---	---	---	---	---	---	---	0.6	---
0.300	0.8*	1.5	1.1	---	---	0.4*	---	---	---	0.3	0.8	0.9	0.4
0.500	0.9*	1.6	1.0	---	---	---	0.8*	---	---	0.5	0.9	1.0	0.5
0.700	0.7	1.3	1.0	---	0.2	0.3	0.7*	---	0.4*	0.6	1.0	0.9	0.6
1.000	0.7	1.0	1.1	---	---	0.3	---	---	0.6*	0.6	1.2	0.8	0.5
1.500	0.8	1.0	1.3	0.6	0.5	0.5	---	---	0.4*	0.5	1.4	0.8	0.5
2.000	0.9	1.0	1.3	0.6	0.7	0.7	0.4	0.4*	0.5*	0.9	1.6	0.9	---
3.000	0.8	0.9	1.2	0.6	0.6	0.9	1.2	0.6*	0.4*	1.3	1.6	1.1	---

Table 10—Amplitude of SC-Like Term (K)

P(hPa)	60S	50S	40S	30S	20S	10S	Eq	10N	20N	30N	40N	50N	60N
0.007	1.4	1.0	1.4	1.0	1.0	---	0.6	---	0.7	1.5	1.2	1.4	1.5
0.010	1.6	0.9	0.8	1.1	0.9	---	1.0	---	1.0	1.7	1.3	1.5	1.5
0.015	1.5	1.0	0.9	0.8	1.0	---	1.1	---	1.1	2.0	1.6	1.6	1.7
0.020	1.7	0.8	1.1	0.7	1.2	---	---	---	1.4	2.1	1.6	1.6	1.7
0.030	1.7	1.0	1.3	0.9	1.0	0.9	0.5	0.5	1.0	1.7	1.0	1.1	1.7
0.050	1.9	---	1.3	1.0	0.5	0.5	1.1	---	---	---	---	---	1.3
0.070	1.9	---	1.6	1.2	0.4	---	0.9	0.6	---	---	---	---	1.0
0.100	1.5	---	1.6	1.0	0.4	---	---	---	---	---	---	---	0.5
0.150	1.2	---	1.3	0.6	---	---	---	0.5	---	---	---	---	---
0.200	1.1	---	1.2	0.4	---	0.3	0.4	0.5	---	---	0.8	0.8	0.3
0.300	1.0	---	0.7	0.3	---	---	---	0.2	---	---	1.0	0.8	0.3
0.500	0.8	---	---	---	0.4	---	---	0.2	0.5	0.5	0.8	---	0.7
0.700	1.0	---	---	0.4	0.4	0.4	0.5	0.5	0.4	0.4	0.6	---	0.7
1.000	0.9	0.7	---	---	0.5	0.3	0.7	0.5	0.4	---	0.3	---	0.6
1.500	0.8	---	---	0.3	0.5	0.3	0.6	0.5	0.5	---	---	---	0.5
2.000	0.7	---	0.5	---	0.5	0.5	0.5	0.4	0.6	0.5	0.4	---	0.6
3.000	0.4	---	0.5	---	0.5	0.8	0.7	0.7	0.7	0.7	0.6	---	0.8

Table 11—Time of Maximum (in yrs) Past 1 January 1991 for SC Term

P(hPa)	60S	50S	40S	30S	20S	10S	Eq	10N	20N	30N	40N	50N	60N
0.007	8.9	10.9	8.9	9.3	10.3	---	8.2	---	0.4	0.4	0.2	0.2	0.3
0.010	8.7	10.6	10.1	9.1	10.9	---	7.0	---	0.6	0.6	0.5	0.1	10.9
0.015	8.2	10.8	10.6	10.1	1.1	---	6.7	---	1.0	0.8	0.7	0.0	10.5
0.020	8.0	0.0	10.7	0.3	1.4	---	---	---	1.3	1.1	0.9	0.1	10.4
0.030	7.6	0.0	10.7	0.5	1.8	0.8	1.5	0.4	1.0	1.1	1.3	0.1	10.2
0.050	6.9	---	10.6	0.3	1.1	0.4	1.2	---	---	---	---	---	10.3
0.070	7.1	---	10.4	10.7	0.0	---	1.3	2.8	---	---	---	---	10.3
0.100	7.7	---	10.3	10.6	10.2	---	---	---	---	---	---	---	10.5
0.150	8.4	---	9.9	10.1	---	---	---	10.4	---	---	---	---	---
0.200	8.9	---	9.6	9.7	---	0.7	0.2	9.8	---	---	9.2	10.0	1.2
0.300	9.3	---	9.1	9.8	---	---	---	8.4	---	---	9.7	9.9	1.9
0.500	10.4	---	---	---	9.9	---	---	1.7	0.0	9.8	10.1	---	2.0
0.700	0.0	---	---	8.0	9.5	0.9	1.0	1.8	10.6	9.3	10.4	---	2.5
1.000	0.0	0.0	---	---	10.1	0.9	0.5	1.1	9.2	---	10.5	---	2.9
1.500	10.3	---	---	1.6	10.8	10.2	0.5	10.9	8.6	---	---	---	3.9
2.000	10.0	---	4.1	---	10.0	9.5	10.5	9.6	8.7	10.1	10.4	---	4.5
3.000	9.3	---	5.4	---	8.5	8.7	9.0	8.5	8.7	9.3	9.0	---	5.2

Table 12—Linear Trend Term (K/decade)

P(hPa)	60S	50S	40S	30S	20S	10S	Eq	10N	20N	30N	40N	50N	60N
0.007	-2.3	-0.9	-2.0	---	---	---	-1.0	---	---	---	---	-1.2	---
0.010	-2.1	-1.1	---	---	---	---	-0.9	---	---	---	-0.7	-1.6	---
0.015	-1.6	-1.7	-0.8	---	---	---	-0.9	---	---	-1.2	-1.6	-2.6	---
0.020	-1.3	-1.4	-1.5	---	-0.6	---	---	---	---	-1.7	-2.1	-3.1	---
0.030	-0.8	-1.5	-1.7	-0.8	---	---	---	---	---	-1.6	-2.3	-3.3	---
0.050	---	-1.3	-1.4	-1.4	-0.8	---	---	---	---	-1.0	-2.0	-2.5	---
0.070	---	-1.1	-1.6	-1.5	-1.3	---	---	---	---	-1.4	-1.7	-2.1	---
0.100	-0.8	-1.0	-2.0	-1.3	-1.2	---	---	---	---	-1.1	-1.2	-1.5	---
0.150	-1.0	---	-1.7	-0.7	---	---	---	---	-0.8	---	---	-0.5	---
0.200	-0.7	---	-1.4	---	---	---	---	---	-0.7	---	---	-0.6	---
0.300	-0.7	---	-0.8	---	---	---	---	---	-0.4	---	---	-0.3	---
0.500	---	---	---	---	-0.5	-0.5	---	---	---	---	---	---	---
0.700	-0.6	---	---	---	-0.7	---	-0.8	---	---	---	---	---	---
1.000	-0.5	---	---	-0.6	-0.6	---	---	---	---	---	---	---	---
1.500	-0.9	---	---	-0.5	-0.4	---	---	-0.5	---	---	---	---	---
2.000	-1.2	---	---	-0.8	-1.1	-0.9	-0.8	-0.8	-0.8	-1.1	-0.5	---	---
3.000	-1.5	-1.1	-1.1	-1.3	-1.3	-1.4	-1.1	-1.0	-1.3	-1.6	-0.8	---	---

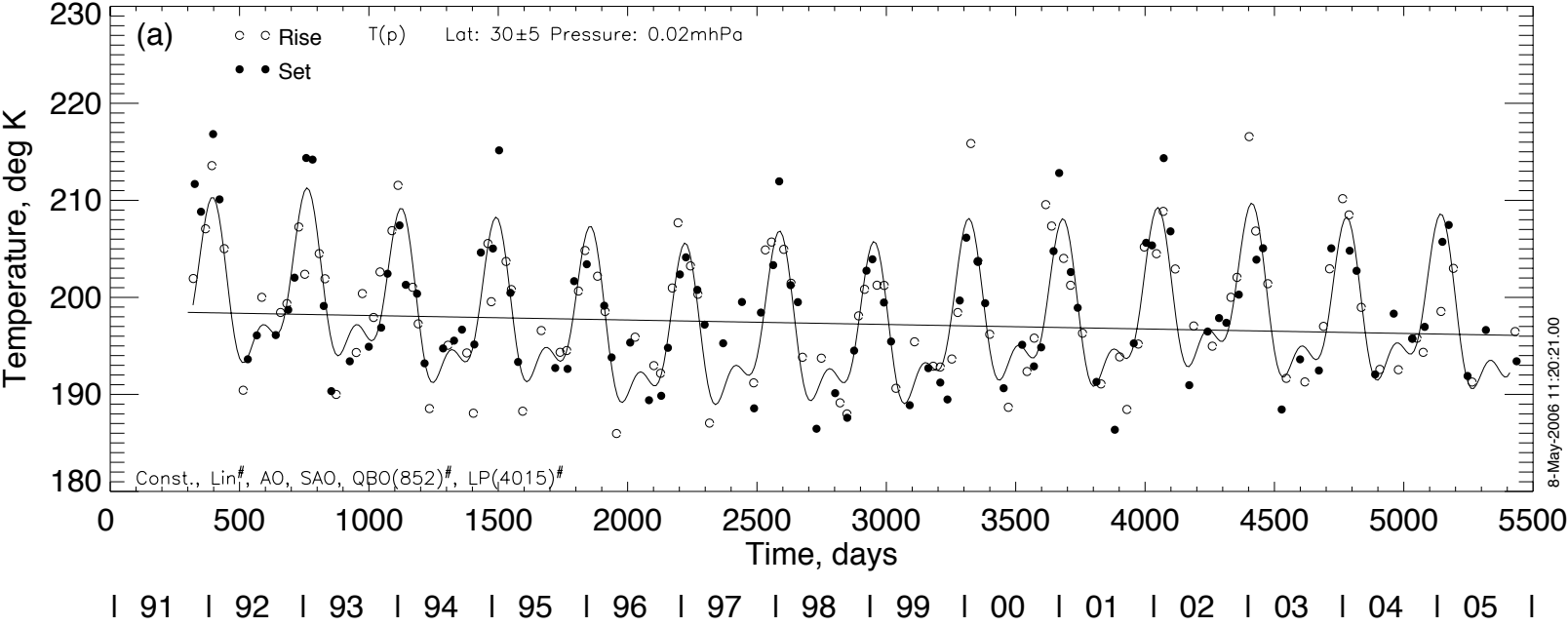
(a)
Rise
Set
T(p)
Lat: 30±5 Pressure: 0.02mhPa
Temperature, deg K
230
220
210
200
190
180
Const., Lin#, AO, SAO, QBO(852)#, LP(4015)#
0
500
1000
1500
2000
2500
3000
3500
4000
4500
5000
5500
Time, days
8-May-2006 11:20:21.00
91
92
93
94
95
96
97
98
99
00
01
02
03
04
05

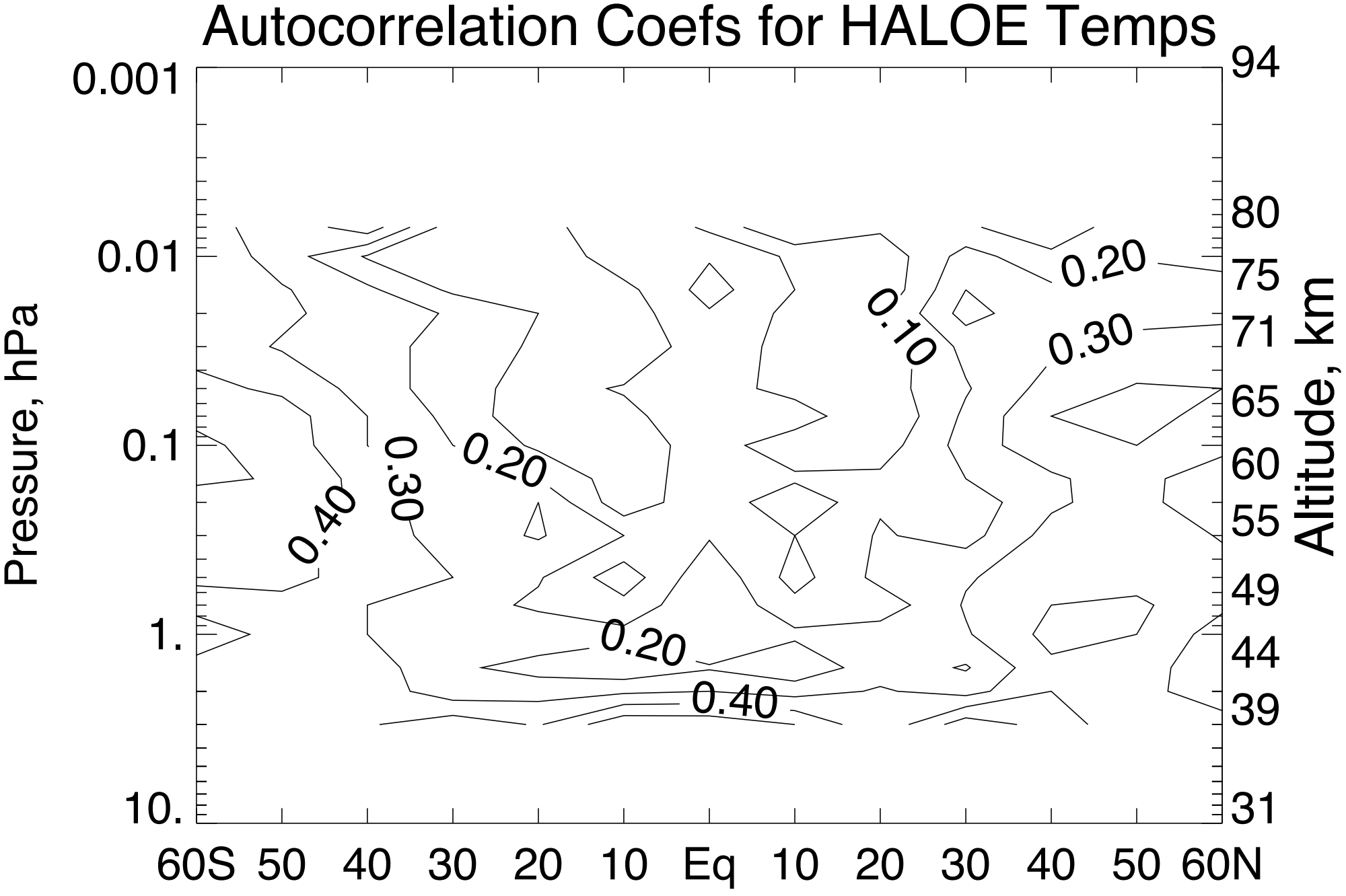
Autocorrelation Coefs for HALOE Temps
Pressure, hPa
0.001
0.01
0.1
1.
10.
Altitude, km
94
80
75
71
65
60
55
49
44
39
31
0.40
0.30
0.20
0.10
0.20
0.30
0.20
0.40
60S 50 40 30 20 10 Eq 10 20 30 40 50 60N

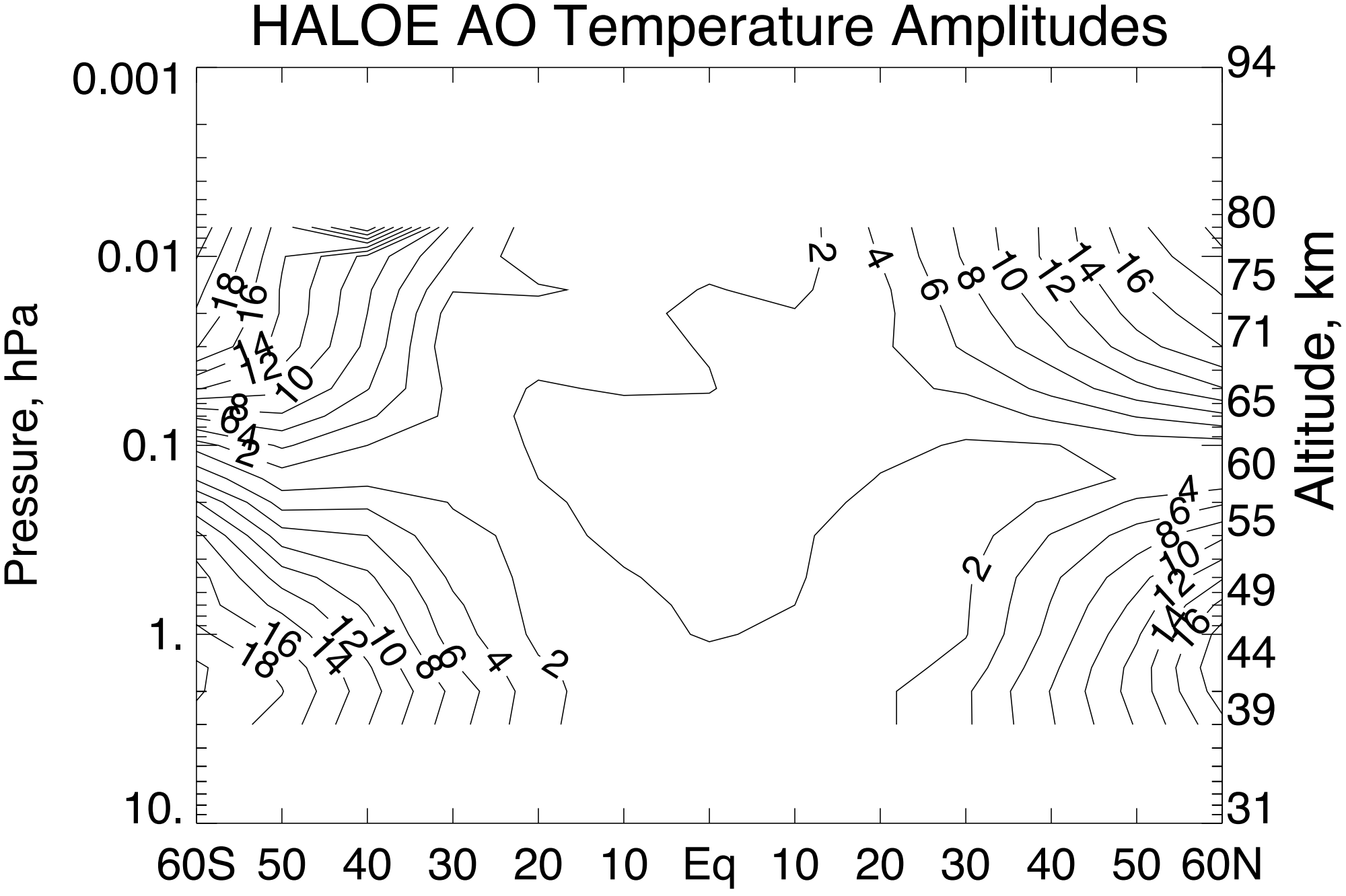
HALOE AO Temperature Amplitudes
Pressure, hPa
0.001
0.01
0.1
1.
10.
Altitude, km
94
80
75
71
65
60
55
49
44
39
31
60S 50 40 30 20 10 Eq 10 20 30 40 50 60N

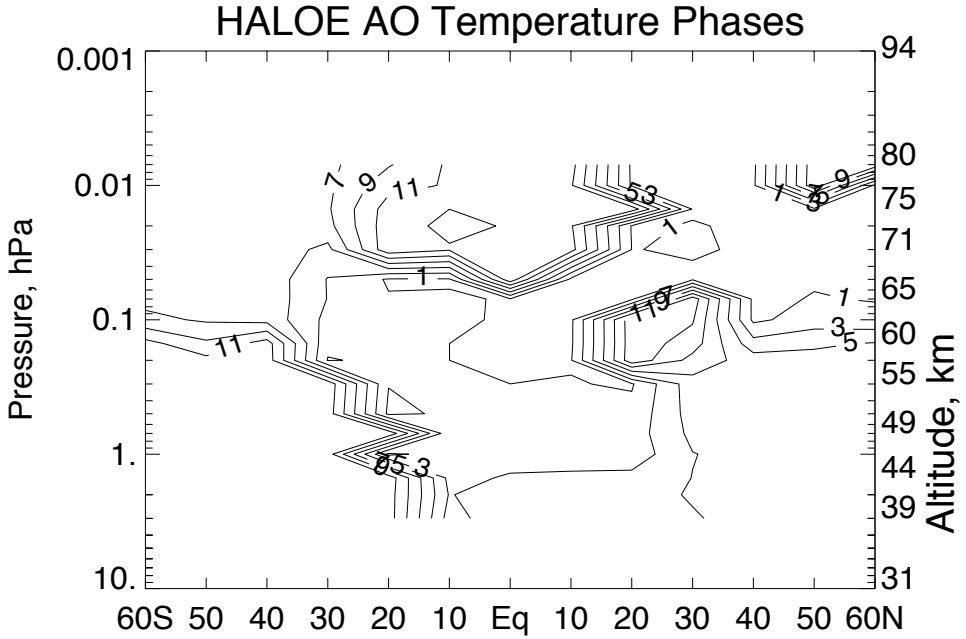
HALOE AO Temperature Phases
Pressure, hPa
0.001
0.01
0.1
1.
10.
Altitude, km
94
80
75
71
65
60
55
49
44
39
31
60S 50 40 30 20 10 Eq 10 20 30 40 50 60N

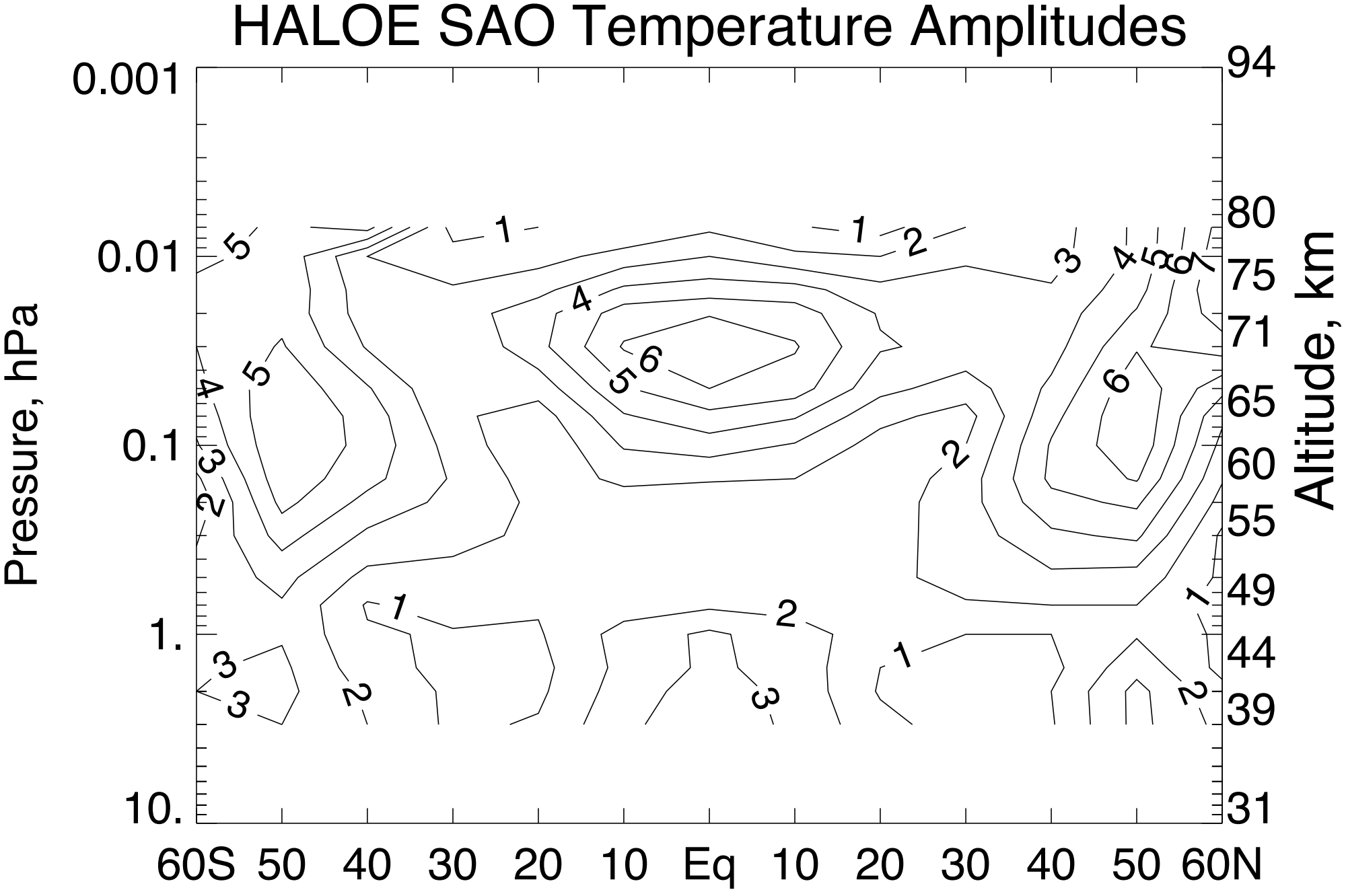
HALOE SAO Temperature Amplitudes
Pressure, hPa
0.001
0.01
0.1
1.
10.
Altitude, km
94
80
75
71
65
60
55
49
44
39
31
60S 50 40 30 20 10 Eq 10 20 30 40 50 60N

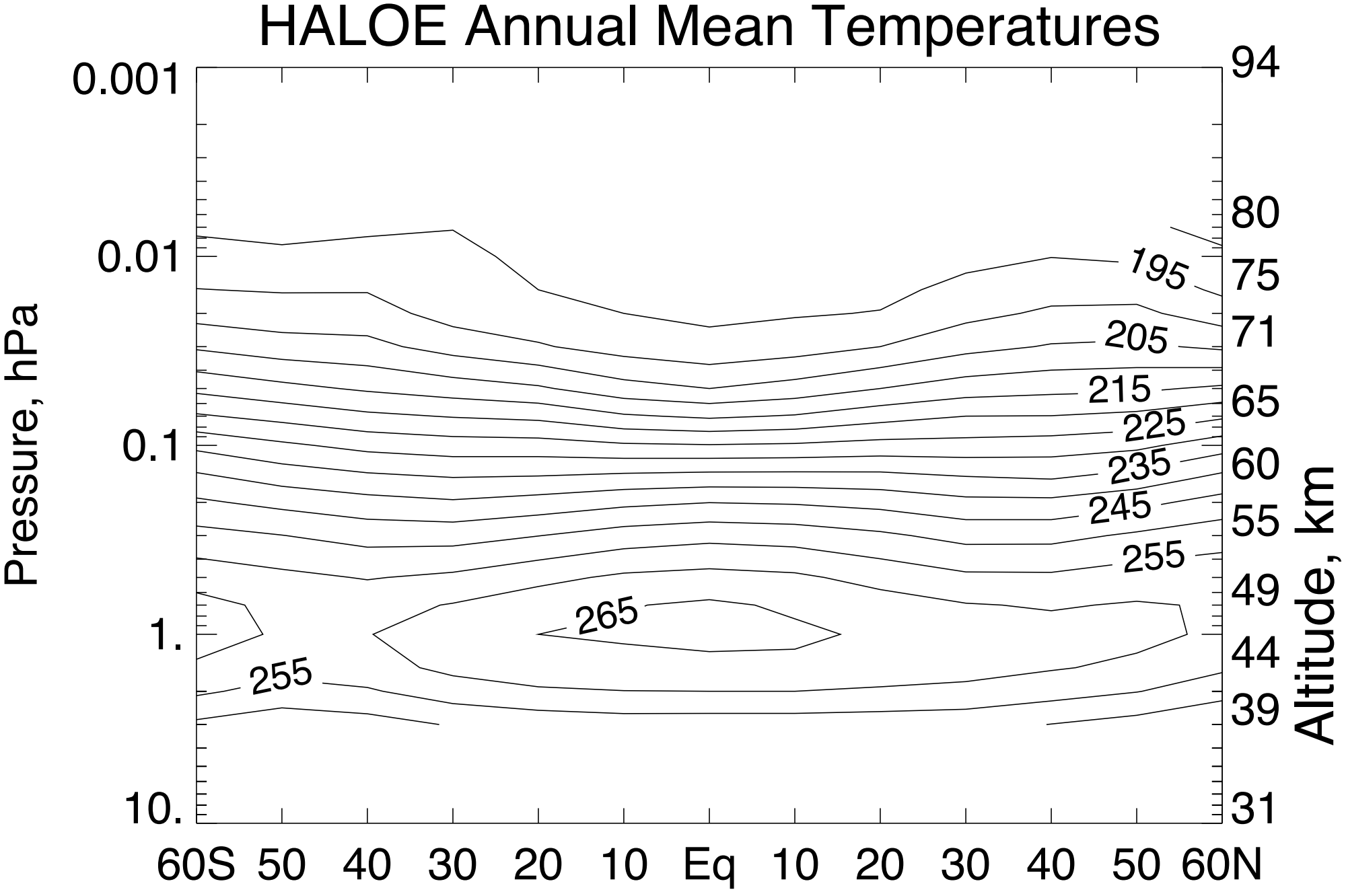
HALOE Annual Mean Temperatures
Pressure, hPa
0.001
0.01
0.1
1.
10.
Altitude, km
94
80
75
71
65
60
55
49
44
39
31
195
205
215
225
235
245
255
265
255
60S 50 40 30 20 10 Eq 10 20 30 40 50 60N

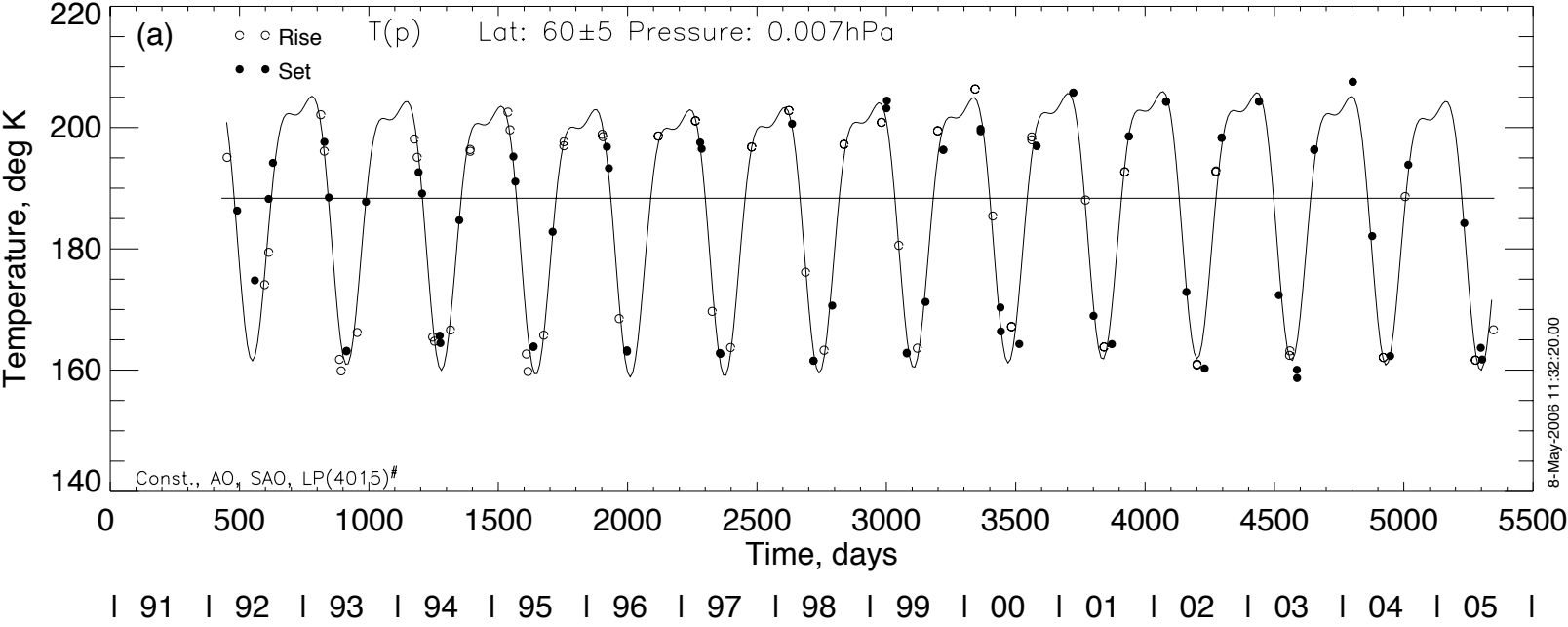
(a)
Rise
Set
T(p)
Lat: 60±5 Pressure: 0.007hPa
Temperature, deg K
220
200
180
160
140
Const., AO, SAO, LP(4015)#
0
500
1000
1500
2000
2500
3000
3500
4000
4500
5000
5500
Time, days
8-May-2006 11:32:20.00
91
92
93
94
95
96
97
98
99
00
01
02
03
04
05

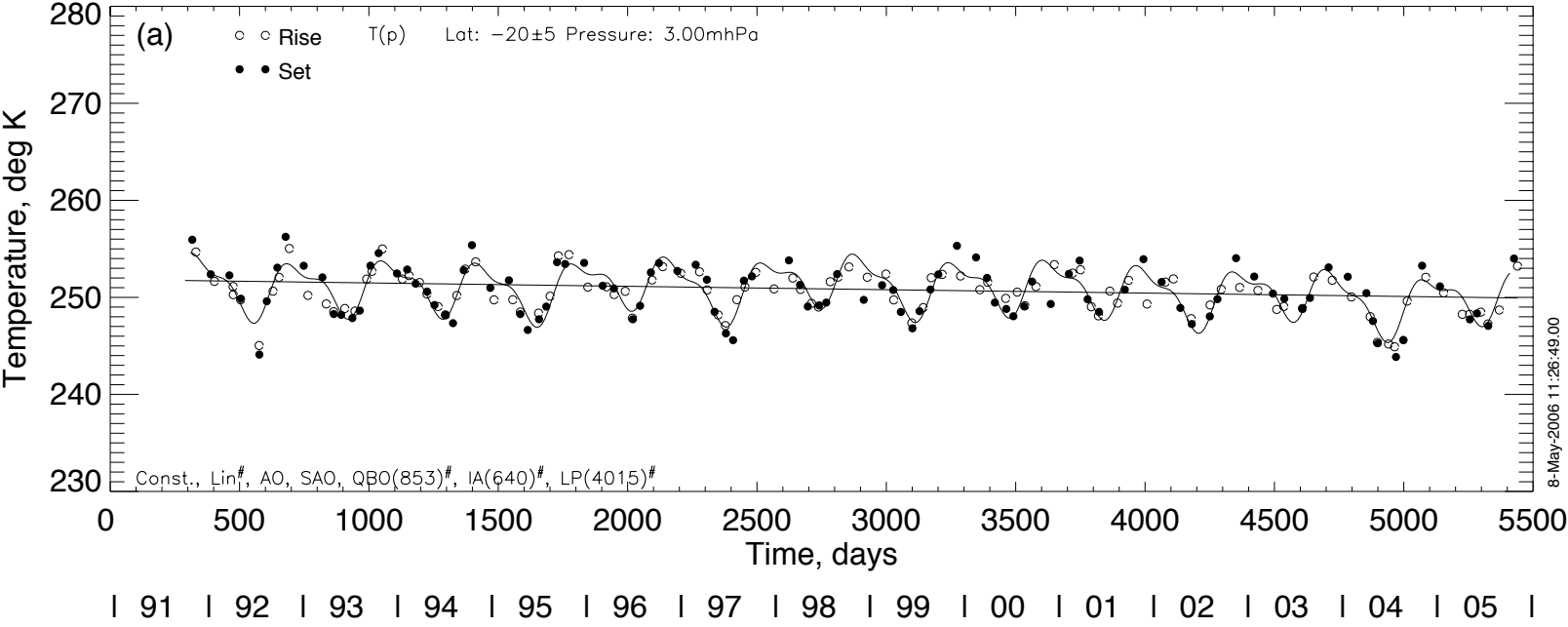
(a)
Rise
Set
T(p)
Lat: −20±5 Pressure: 3.00mhPa
Temperature, deg K
280
270
260
250
240
230
Const., Lin#, AO, SAO, QBO(853)#, IA(640)#, LP(4015)#
8-May-2006 11:26:49.00
0
500
1000
1500
2000
2500
3000
3500
4000
4500
5000
5500
Time, days
91
92
93
94
95
96
97
98
99
00
01
02
03
04
05

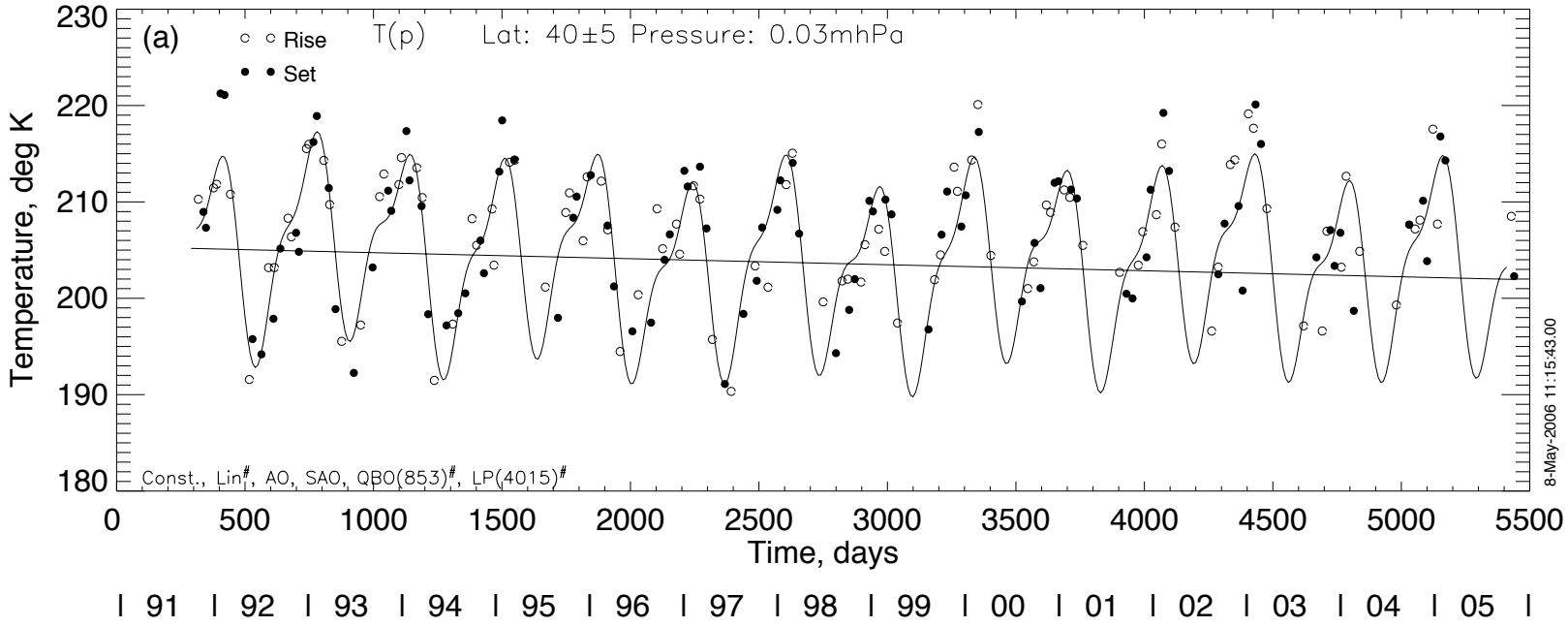
(a)
Rise
Set
T(p)
Lat: 40±5 Pressure: 0.03mhPa
Const., Lin#, AO, SAO, QBO(853)#, LP(4015)#
Temperature, deg K
230
220
210
200
190
180
0
500
1000
1500
2000
2500
3000
3500
4000
4500
5000
5500
Time, days
8-May-2006 11:15:43.00
91
92
93
94
95
96
97
98
99
00
01
02
03
04
05

HALOE SC MAX MINUS MIN T(P) IN (K)

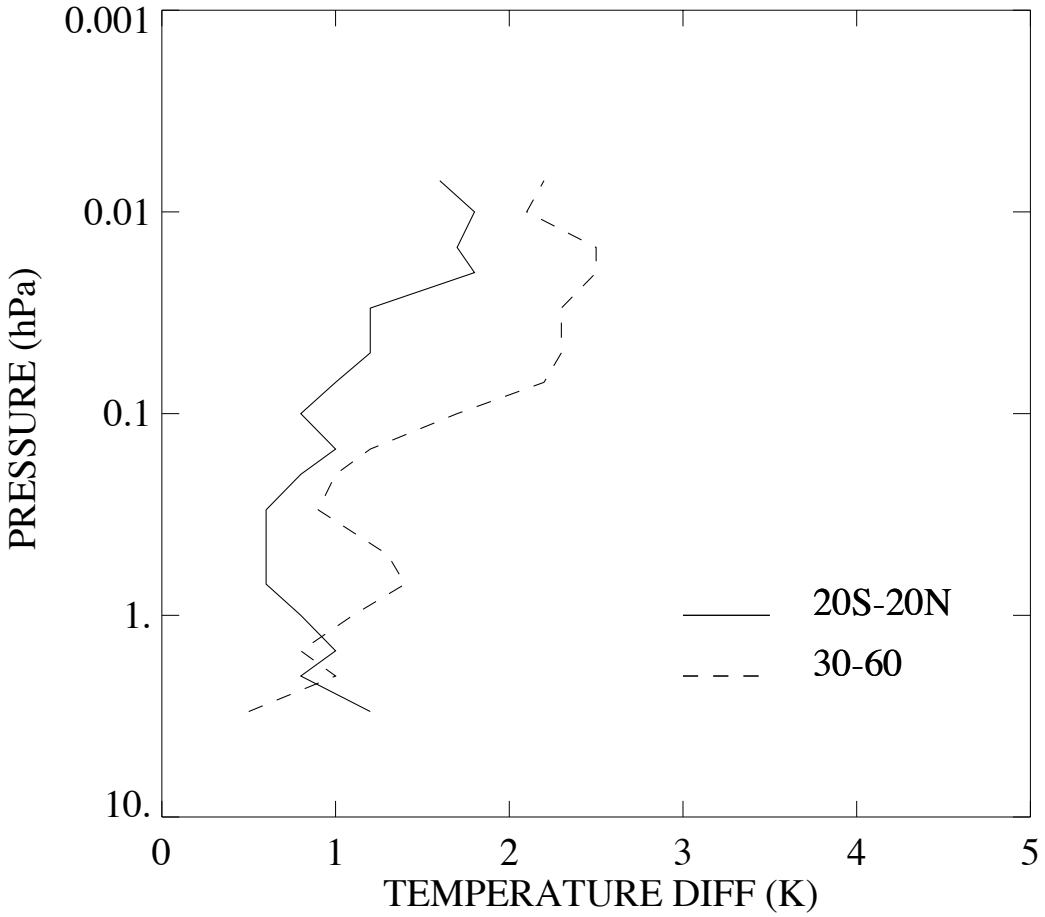

HALOE TREND IN T(P)